

# Multiple critical point structure for chiral phase transition induced by charge neutrality and vector interaction

Zhao Zhang and Teiji Kunihiro

Department of Physics

Kyoto University

Kyoto 606-8502

Japan

Email: zhaozhang@pku.org.cn

The combined effect of the repulsive vector interaction and the positive electric chemical potential on the chiral phase transition is investigated by considering neutral color superconductivity. Under the charge-neutrality constraint, the chiral condensate, diquark condensate and quark number densities are obtained in two-plus-one-flavor Nambu-Jona-Lasinio model with the so called Kobayashi-Maskawa-'t Hooft term. We demonstrate that multiple chiral critical-point structures always exist in the Nambu-Jona-Lasinio model within the self-consistent mean-field approximation, and that the number of chiral critical points can vary from zero to four, which is dependent on the magnitudes of vector interaction and the diquark coupling.

## I. INTRODUCTION

It is generally believed that QCD exhibits a rich phase structure in an extreme environment such as at high temperature and high baryon chemical potential. For the chiral phase transition, it is a widely accepted view that the critical point(s) (i.e. the end point of the first-order phase boundary) should exist at finite temperature and density. Usually, a schematic  $T$ - $\mu$  phase diagram with one critical point is widely adopted in the literature [1].

The color-superconducting (CSC) phase may appear in the  $T$ - $\mu$  phase diagram of QCD for low temperature and large baryon chemical potential [2–5]. At asymptotically high density that justifies the perturbative QCD calculations, the color-flavor locked (CFL) phase [6] has been established as the ground state of quark matter. For the intermediate density region which may exist in the core of a compact star, the nonperturbative features of QCD play a more important role in the phase structure of QCD, and both CFL and non-CFL CSC phases may manifest themselves in this region.

The appearance of the CSC phase around the boundary of the chiral phase transition at low temperatures should affect the chiral phase transition, which may result in an unexpected phase structure of QCD. Especially, the competition between the chiral condensate and the diquark condensate may lead to the emergence of the new chiral critical point(s) in the low temperature region. Such an example was first presented in [7] in a two-flavor Nambu-Jona-Lasinio (NJL) model with the vector interaction: It was found that the repulsive vector interaction can lead to a two-critical-point structure in the  $T$ - $\mu$  phase diagram of QCD. The appearance of the new critical point is attributed to the fact that the density-density correlation induced by the vector interaction effectively enhances the competition mentioned above while weakening the first-order chiral restoration. For the three flavor case, the realization of a similar QCD phase diagram has been recently conjectured [8], where the  $U_A(1)$ -breaking vertex may induce a new critical point in the low temperature region. This conjecture is based on a general Ginzburg-Landau theory constrained by QCD symmetries and the CFL phase is assumed to appear near the chiral boundary in the  $SU_f(3)$  limit. It has been argued that the resultant crossover of the chiral restoration at small temperatures embodies the hadron-quark continuity hypothesis [9].

Note that the two-critical point structures obtained above are all based on the exact flavor symmetry. Namely, the quarks with different flavor have the same mass and density. In realistic situations,  $s$  quark is much heavier than  $u$  and  $d$  quarks, which may make a different phase structure involving the chiral transition. In particular, the large mass difference between  $s$  quark and  $u(d)$  quark may disfavor the formation of the CFL in the intermediate density region. Thus, the conjecture of the two-critical-point structure claimed in [8] may not be true in the realistic situation. In addition, near the chiral boundary, even though the mass difference between the  $u$  quark and the  $d$  quark is very small in contrast to the quark chemical potential, the constraint by local electric-charge neutrality may lead to a relatively large density disparity between them. In short, we can expect that the Fermi sphere differences among  $u$ ,  $d$  and  $s$  quarks should have significant influence on the chiral phase transition in the presence of CSC.

Considering the local charge neutrality constraint, it was first disclosed in [10] that the positive electric chemical potential  $\mu_e$  plays a similar role on the chiral transition as the repulsive vector interaction. This is another mechanism which can realize a multiple chiral critical-point structure. In a simple two-flavor NJL model, the same two-critical-point structure found in [7] can be realized without introducing vector interaction when taking into account the local electric-neutrality [10]. Moreover, besides its role as an effective vector interaction, the positive  $\mu_e$  also implies a finite disparity between Fermi spheres of  $u$  and  $d$  quarks. For a system composed of two different Fermions with the mismatched Fermi spheres, it is known that the energy gap of the Cooper pairing between them can *increase* with temperature. This unusual thermal behavior is due to the smearing of the Fermi surface by the temperature. Such an unconventional behavior in the two-flavor neutral CSC phase can lead to a special competition between the chiral condensate and the diquark condensate, which may be enhanced with increasing temperature. For some model parameter regions, this abnormal competition can give rise to *three* chiral critical structure in the phase diagram [10]. We remark that the interplay of two order parameters with the external constraint(s) should be a general mechanism for a realization of a multiple critical-point structure in many-body system including those in condensed matter physics.

It is an interesting problem whether the multiple critical-point structure can appear in the QCD phase diagram for the two-plus-one-flavor case. The CFL phase may be disfavored near the chiral boundary in this case due to the relatively heavy strange quark. In addition, the  $U_A(1)$  anomaly of QCD may have significant influence on the chiral phase transition. Such an anomaly can be successfully fulfilled in the effective quark field theory with the so-called Kobayashi-Maskawa-'t Hooft(KMT) term[11]. Because of the similar roles of the repulsive vector interaction and the electric chemical potential under the neutrality constraint on the chiral phase transition, it is naturally expected that chiral restoration is weakened more significantly when taking into account both aspects simultaneously. The study of the QCD phase diagram including all these ingredients has been done in [12] in the framework of a two-plus-one-flavor NJL model.

As we will show below, the multiple chiral critical point structures can still emerge in the QCD phase diagram for the two-plus-one-flavor case. Such a conclusion is qualitatively different from the result in [13, 14] where the same model was used without considering the vector interaction. This just reflects the combined effect of the electric chemical potential and vector interaction on the chiral phase transition through a special competition of the chiral condensate and the diquark condensate. It should be stressed that the present mechanism giving rise to the multiple chiral critical structures is different from that reported in [8] where the anomaly term in the flavor- $SU(3)$  limit plays the essential role. In our case, only two-flavor CSC (2CSC) phase appears near the chiral boundary and there is no cubic interactions between the chiral condensate and the diquark condensate and the number of the chiral critical points can be more than two.

$m_{u,d}(\text{MeV})$	$m_s(\text{MeV})$	$G_S \Lambda^2$	$K \Lambda^5$	$\Lambda$ (MeV)	$M_{u,d}$ (MeV)
5.5	140.7	1.835	12.36	602.3	367.7
$f_\pi(\text{MeV})$	$m_\pi(\text{MeV})$	$m_K$ (MeV)	$m_\eta$ (MeV)	$m_\eta(\text{MeV})$	$M_s$ (MeV)
92.4	135	497.7	957.8	514.8	549.5

TABLE I: Model parametrization of the two-plus-one-flavor NJL model.

## II. TWO-PLUS-ONE-FLAVOR NJL MODEL

In this part, for simplicity, a local two-plus-one-flavor NJL model is adopted to investigate the QCD critical-point structure. The two-plus-one-flavor NJL model was developed in the mid-1980s [15–17], and the most popular version includes a chiral symmetric four-quark interaction term and a determinantal term [11] in flavor space [18–20]. To compare with the previous study, we take the same model parameters as in Ref.[13] by including the vector interaction channel. The corresponding Lagrangian density is given by

$$\begin{aligned} \mathcal{L} = & \bar{\psi}(i\not{\partial} - \hat{m})\psi + G_S \sum_{i=0}^8 \left[ (\bar{\psi}\lambda_i\psi)^2 + (\bar{\psi}i\gamma_5\lambda_i\psi)^2 \right] + G_D \sum_{\gamma,c} \left[ \bar{\psi}_\alpha^a i\gamma_5 \epsilon^{\alpha\beta\gamma} \epsilon_{abc} (\psi_C)_\beta^b \right] [(\bar{\psi}_C)_\rho^r i\gamma_5 \epsilon^{\rho\sigma\gamma} \epsilon_{rsc} \psi_\sigma^s] \\ & - G_V \sum_{i=0}^8 \left[ (\bar{\psi}\gamma^\mu\lambda_i\psi)^2 + (\bar{\psi}i\gamma^\mu\gamma_5\lambda_i\psi)^2 \right] - K \left\{ \det_f [\bar{\psi}(1 + \gamma_5)\psi] + \det_f [\bar{\psi}(1 - \gamma_5)\psi] \right\}, \end{aligned} \quad (1)$$

where the quark spinor field  $\psi_\alpha^a$  carries color ( $a = r, g, b$ ) and flavor ( $\alpha = u, d, s$ ) indices. In contrast to the two-flavor case, the matrix of the quark current masses is given by  $\hat{m} = \text{diag}_f(m_u, m_d, m_s)$  and the Pauli matrices in flavor space are replaced by the Gell-Mann matrices  $\lambda_i$  in flavor space with  $i = 1, \dots, 8$ , and  $\lambda_0 \equiv \sqrt{2/3} \mathbf{1}_f$ . The corresponding parametrization of the model parameters is given in Table I, where  $G_S$ , the coupling constant for the scalar meson channel, and  $K$ , the coupling constant responsible for the  $U_A(1)$  breaking, or the KMT term[11], are fixed by the vacuum physical observables. Because there are no reliable constraints on the coupling constants  $G_V$  and  $G_D$  within the NJL model, these two model parameters are taken as free parameters in our treatment. The standard ratios of  $G_V/G_S$  and  $G_D/G_S$  from Fierz transformation are 0.5 and 0.75, respectively. In addition, in the molecular instanton liquid model, the ratio  $G_V/G_S$  is 0.25. Considering these two points, the reasonable value of  $G_V/G_S$  may be located in the range from 0 to 0.5.

## III. THERMODYNAMIC POTENTIAL FOR NEUTRAL COLOR SUPERCONDUCTIVITY

In general, there exist nine possible two-quark condensates for the two-plus-one-flavor case with the Lagrangian (1): three chiral condensates  $\sigma_\alpha$ , three diquark condensates  $\Delta_c$ , and three vector quark condensates  $\rho_\alpha$ , where  $\alpha$  and  $c$  stand for three flavors and three colors, respectively. In the mean-field level, the thermodynamic potential for the two-plus-one-flavor NJL model including the charge-neutrality constraints, is given by

$$\begin{aligned} \Omega = & \Omega_l + \frac{1}{4G_D} \sum_{c=1}^3 |\Delta_c|^2 - 2G_V \sum_{\alpha=1}^3 \rho_\alpha^2 + 2G_S \sum_{\alpha=1}^3 \sigma_\alpha^2 \\ & - 4K \sigma_u \sigma_d \sigma_s - \frac{T}{2V} \sum_K \ln \det \frac{S_{MF}^{-1}}{T}, \end{aligned} \quad (2)$$

where  $\Omega_l$  stands for the contribution from the free leptons. Note that, for consistency,  $\Omega_l$  should include the contributions from both electrons and muons. Since  $M_\mu \gg M_e$  and  $M_e \approx 0$ , ignoring the contribution from muons has little effect on the phase structure. The corresponding  $\Omega_l$  takes the form

$$\Omega_l = -\frac{1}{12\pi^2} \left( \mu_e^4 + 2\pi^2 T^2 \mu_e^2 + \frac{7\pi^4}{15} T^4 \right). \quad (3)$$

It should be stressed here that, for simplicity, the contributions of the cubic mixing terms among three different condensates, such as  $\sigma\Delta^2$ ,  $\rho\Delta^2$ , and  $\sigma\rho^2$ , are neglected in Eq. (2). These terms arise from the KMT interaction which may or may not affect the phase structure. In particular it was argued in [8] that the cubic mixing term between chiral and diquark condensates may play an important role in the chiral phase transition in the low temperature region. Beside the direct contribution of these cubic terms to the thermodynamic potential, the flavor mixing terms arising from the KMT interaction also have influence on the dispersion relationship of quasi-quarks. For example, both the diquark condensate and the quark number density contribute to the dynamical quark masses. Therefore, it is a very interesting subject to investigate the possible effect of these cubic coupling terms on the phase diagram. Leaving an investigation of this interesting problem to our future work, here we just simply assume that none of these mixing terms makes a qualitative difference in the phase diagram.

Because of the large mass difference between the strange quark and the  $u, d$  quarks, the favored phase at low temperature and moderate density can be most probably the 2CSC phase rather than CFL phase as is demonstrated in the two-plus-one-flavor NJL model [13, 14]. These studies suggest that the strange quark mass is close to or even larger than  $\mu$  near the chiral boundary, which means that the strange quark density is considerably smaller than that of the  $u$  and  $d$  quarks. Therefore, for the two-plus-one-flavor case, the light quarks still play the dominant role at least around the phase boundary of the chiral transition, and the amount of the density difference between the  $u$  and  $d$  quarks under the electric-charge-neutrality constraint is still similar to that in the two-flavor case. Since the main purpose of our study is to investigate the influence of the neutral CSC phase on the chiral phase transition by taking into account the vector interaction, only the 2CSC phase is considered in the following.

The inverse quark propagator  $S_{MF}^{-1}$  in the 2CSC phase for the two-plus-one-flavor case formally takes the same form as that in two-flavor case [12], with the extended matrices  $\hat{\mu}$  and  $\hat{M}$  in the three-flavor space. We refer to [12] for the notations to be used below. The constituent quark mass is given by

$$M_\alpha = m_\alpha - 4G_S\sigma_\alpha + 2K\sigma_\beta\sigma_\gamma, \quad (4)$$

and the effective quark chemical potentials take the form

$$\tilde{\mu}_u = \mu - 4G_V\rho_u - \frac{2}{3}\mu_e, \quad (5)$$

$$\tilde{\mu}_d = \mu - 4G_V\rho_d + \frac{1}{3}\mu_e, \quad (6)$$

$$\tilde{\mu}_s = \mu - 4G_V\rho_s + \frac{1}{3}\mu_e. \quad (7)$$

The average chemical potential between  $u$  quark and  $d$  quark is defined by

$$\bar{\mu} = \frac{\tilde{\mu}_{rd} + \tilde{\mu}_{gu}}{2} = \frac{\tilde{\mu}_{ru} + \tilde{\mu}_{gd}}{2} = \mu - \frac{\mu_e}{6} - 2G_V(\rho_u + \rho_d) + \frac{\mu_8}{3}, \quad (8)$$

and the effective mismatch between the chemical potentials of the  $u$  quark and the  $d$  quark takes the form

$$\delta\tilde{\mu} = \frac{1}{2}(\mu_e - 4G_V(\rho_d - \rho_u)). \quad (9)$$

The quantity  $\tilde{\mu}$  ( $\delta\tilde{\mu}$ ) still has the same form as that in two-flavor case [12].

Note that there are three main changes induced by the nonzero vector-type quark condensates in comparison to the case without vector interactions [10]. First, it gives new negative contributions to the thermal potential, which favors the phase with relatively larger dynamical quark mass. This effect becomes more significant when the quark number density is sizable. Second, it gives rise to a negative dynamical chemical potential, which can delay the chiral restoration towards larger chemical potential to drive the formation of the coexistence (COE) phase with both the  $\chi$ SB and the CSC phase. In the COE region, the competition between the two order parameters can significantly weaken the first-order chiral phase transition. Third, the disparity between the densities of  $u$  and  $d$  quarks can effectively suppress the chemical-potential mismatch between these two flavors, which might partially or even totally cure the chromomagnetic instability. The detailed description on the third point was given in [12].

If the mass difference between the  $u$  and  $d$  quarks is ignored, which is actually an excellent approximation [13]), the last term in Eq. (2) has an analytical form, and hence, the numerical calculation is greatly simplified. Adopting the variational method, we get the eight nonlinear coupled equations

$$\frac{\partial\Omega}{\partial\sigma_u} = \frac{\partial\Omega}{\partial\sigma_s} = \frac{\partial\Omega}{\partial\Delta} = \frac{\partial\Omega}{\partial\rho_u} = \frac{\partial\Omega}{\partial\rho_d} = \frac{\partial\Omega}{\partial\rho_s} = \frac{\partial\Omega}{\partial\mu_e} = \frac{\partial\Omega}{\partial\mu_8} = 0. \quad (10)$$

In fact, since  $\mu_8$  is found to be tiny around the critical point of the chiral transition [13, 14], we can set  $\mu_8 = 0$  without affecting the numerical results in any significant way.

#### IV. NUMERICAL CALCULATION AND DISCUSSION

To investigate the influence of the vector interaction on the chiral phase transition, the coupling  $G_V/G_S$  is taken as a free parameter in the following, and the diquark coupling  $G_D/G_S$  is fixed to the standard value. Because of the contribution from the six-quark KMT interaction, the ratio  $G_D/G_S$  obtained by Fierz transformation should be 0.95 rather than 0.75 in the case where only the four-quark interaction is considered[4]: In this case, the effective four-quark interaction which determines the quark constituent mass in vacuum is  $G_{S'} = G_S - \frac{1}{2}K\sigma_s$ , and the standard value of  $G_D/G_{S'}$  should be 0.75.

For convenience, the same notations as those in Refs. [8, 10] are adopted to distinguish the different regions in the  $T$ - $\mu$  phase diagram of QCD: NG, CSC, COE, and NOR refer to the hadronic (Nambu-Goldstone) phase with  $\sigma \neq 0$  and  $\Delta = 0$ , the color-superconducting phase with  $\Delta \neq 0$  and  $\sigma = 0$ , the coexisting phase with  $\sigma \neq 0$  and  $\Delta \neq 0$ , and the normal phase with  $\sigma = \Delta = 0$ , respectively, though they only have exact meanings in the chiral limit.

The phase diagrams with a multiple critical-point structure are shown in Fig. 1 for various strengths of the vector interaction. As the vector interaction becomes large, the traditional one critical-point structure is replaced by the two critical-point structure and a new critical point at a very low temperature emerges. Such a two critical-point structure of the QCD phase diagram was first suggested or conjectured in [7] and [8], respectively. With a further increase of the vector interaction, a four critical-point structure manifest itself in the phase diagram, which is a quite new findings. The mechanism for realizing such an unusual structure is traced back to the nonzero  $\mu_e$ , which leads to the abnormal thermal behavior of the diquark condensate in the COE region. The phase structure with more than two critical points was first obtained in [10]. With a still further

increase of  $G_V$ , the number of the chiral critical points is reduced to two from four because of the more strong competition between the chiral condensate and diquark condensate. When  $G_V$  is large enough, the chiral transition will totally become crossover and there is no critical point in the phase diagram. Fixing the ratio  $G_D/G_S$  as its standard value, the numerical calculation shows that there appear five types of critical-point structure when the ratio of  $G_V/G_S$  varying from zero to its standard value 0.5.

Note that these phase diagrams are very similar to Fig. 4 in [12], which was obtained in a nonlocal two-flavor NJL model. Actually, these two models almost reproduce the same constituent quark ( $u$  and  $d$ ) masses and have similar scale parameters. It reflects that the strange quark plays only a minor role for the critical properties of the chiral phase transition. Figure 1 shows that the KMT interaction does not alter the possible multiple critical-point structures for the chiral phase transition.

It is noteworthy that the vector interaction acts so as to suppress the chromomagnetic instability of the gapless phases. For simplicity, the unstable regions with chromomagnetic instability are not plotted in Fig.1. The calculation of the Meissner mass squared in the 2CSC phase for the two-plus-one-flavor case is straightforward but complicated. Including the  $s$  quark should have little effect on the value of the Meissner masses calculated according to the formula for the two-flavor case [21] since the  $s$  quark does not take part in the Cooper pairing. We can expect that the critical points E, F, and G should be free from the chromomagnetic instability, as in Fig. 4 for the two-flavor case [12], since the large strange quark mass may give a positive contribution rather than a negative one to the Meissner masses squared. As for critical point H, it might be located in the unstable region but could be safe from the instability because the relatively large  $G_V/G_S$  may shift the unstable region to lower  $T$  and higher  $\mu$ .

Usually, it is argued that the instantons should be screened at large chemical potential and temperature. Therefore, compared to its vacuum value, the coupling constant  $K$  is expected to be reduced around the chiral boundary. For smaller  $K$ , the flavor mixing effect is suppressed and the mass mismatch between the  $s$  quark and the  $u(d)$  quark becomes larger. Accordingly, the influence of the  $s$  quark on the chiral restoration is weakened, and the situation approaches the two-flavor case. On the other hand, with decreasing  $K$ , the  $u(d)$  quark mass also decreases since the contribution from the  $s$  quark mass is reduced. This means that the first-order chiral restoration will be weakened when  $K$  is decreased. Correspondingly, the COE region should be more easily formed with the combined influence of the vector interaction and the neutral CSC phase, which favors the multiple critical-point structures or crossover for chiral restoration at low temperature.

Of course, the produced  $u(d)$  quark vacuum constituent masses with different model parameters of the two-plus-one-flavor NJL model may range from 300-400 MeV, which are all phenomenologically acceptable just as in the two-flavor case. Then, one can expect that all the critical-point structures found in the two-flavor case (the Sec. II of [12]) should also appear in the two-plus-one-flavor case, even when considering the axial anomaly interaction term.

## V. CONCLUSIONS AND OUTLOOK

The vector-vector interaction and electric-charge neutrality in  $\beta$  equilibrium have important effects on the chiral phase transition. In the presence of color superconductivity(CSC), as demonstrated in [12] within the NJL model, the QCD phase diagram may have a multiple chiral critical-point structure. The emergence of such a multiple critical-point structure is made robust with the inclusion of the repulsive vector coupling  $G_V$  between quarks, and it becomes that there always exists a parameter window in the NJL models which favors the appearance of a multiple chiral critical-point structure for a wide range of the vacuum quark mass, i.e., from 300 MeV to 400 MeV [12]. More precisely, besides the two- and three-critical-points structures found in [7, 10] and [10], respectively, the QCD phase diagram can have even *four* critical points; such a multiple critical-point structure is

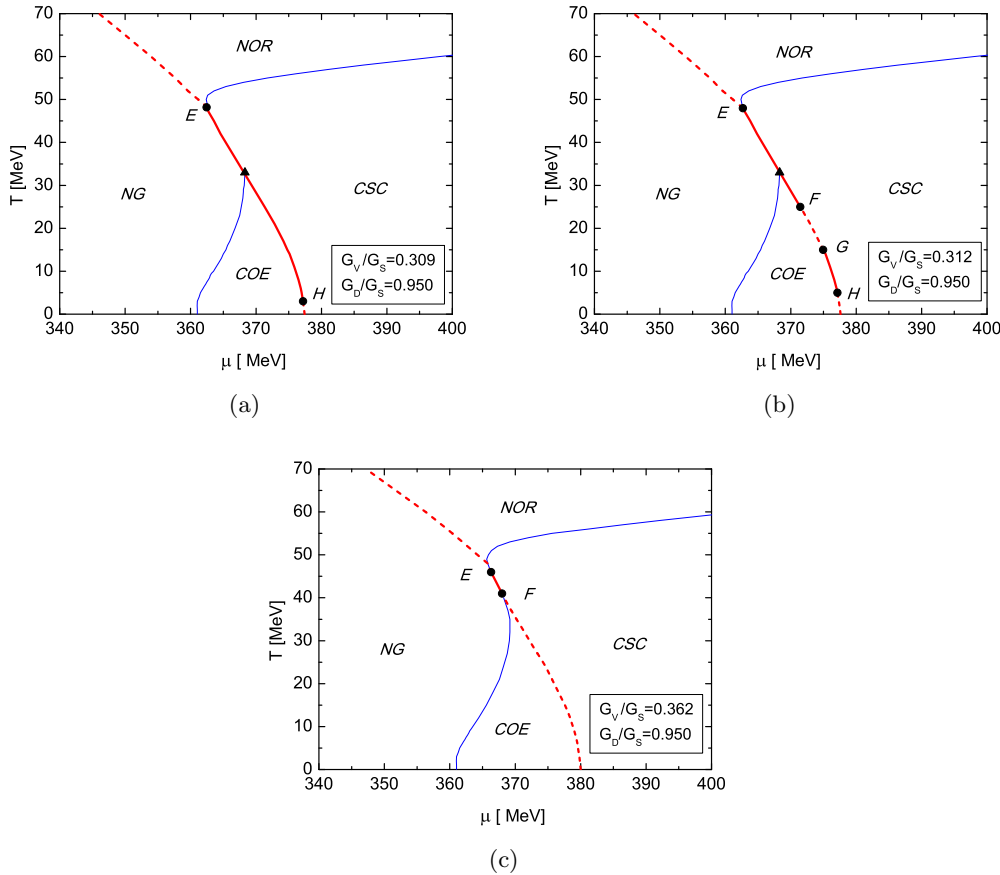


FIG. 1: The phase diagrams for the two-plus-one-flavor NJL model with varying  $G_V/G_S$  and fixed  $G_D/G_S = 0.95$ . Electric-charge-neutrality is taken into account, and only the phase diagrams with multiple chiral critical points are shown.

caused by the combined effect of the positive  $\mu_e$  and  $G_V$ . Because the dynamical strange quark mass is still relatively large near the boundary of the chiral transition, the multiple critical-point structures found in the two-flavor case also appear in the two-plus-one-flavor case. For the intermediate diquark coupling, the number of critical points changes as  $1 \rightarrow 2 \rightarrow 4 \rightarrow 2 \rightarrow 0$  with an increasing vector coupling in the two-plus-one-flavor NJL model. In general, one can expect that different model parameters may possibly give other order of the number of the critical points as the vector coupling is increased.

Although our analysis is based on a low-energy effective model which inherently has, more or less, a parameter dependence, we have seen that the physical mechanism to realize the multiple critical-point structure is solely dependent on the basic ingredients of the effective quark dynamics and thermodynamics. Therefore, we believe that the results obtained in the present work should be taken seriously and examined in other effective models of QCD, or hopefully lattice QCD simulations.

Our result also has a meaningful implication for the study of phase transitions in condensed matter physics. That means some external constraints enforced on the system can lead to the formation or expansion of the coexisting phase, and the competition between two order parameters can give rise to multiple critical points.

Last but not least, in [12] we have shown for the first time that the repulsive vector interaction does suppress the chromomagnetic instability related to the asymmetric homogeneous 2CSC phase. Even such a conclusion is based on a nonlocal two-flavor NJL model, it should also be true for the two-plus-one-flavor case because of the relatively large mass of  $s$  quark. With increasing vector interaction, the unstable region associated with chromomagnetic instability shrinks towards lower temperatures and higher chemical potentials. This means that the vector interaction can partially or even totally resolve the chromomagnetic instability problem.

To cure the chromomagnetic instability, inhomogeneous asymmetric color superconductivity phases such as the LOFF phase and the gluonic phase were proposed in the literature. For the inhomogeneous phase, beside the condensate  $\langle \bar{\psi}\gamma_0\psi \rangle$ , there is no reason to rule out the appearance of another new condensate,  $\langle \bar{\psi}\vec{\gamma}\psi \rangle$ , when considering the vector interaction. The effect of both the timelike vector condensate and the spacelike condensate on the asymmetric inhomogeneous CSC phase will be reported in our future work.

### Acknowledgments

One of the authors ( Z. Z. ) is grateful for the support from the Grants-in-Aid provided by Japan Society for the Promotion of Science (JSPS). This work was partially supported by a Grant-in-Aid for Scientific Research by the Ministry of Education, Culture, Sports, Science and Technology (MEXT) of Japan (No. 20540265 and No. 19-07797), by Yukawa International Program for Quark-Hadron Sciences, and by the Grant-in-Aid for the global COE program “ The Next Generation of Physics, Spun from Universality and Emergence ” from MEXT.

- 
- [1] As a review, see, M. A. Stephanov, Prog. Theor. Phys. Suppl. **153**, 139 (2004) [Int. J. Mod. Phys. A **20**, 4387 (2005)]; PoS **LAT2006**, 024 (2006) [arXiv:hep-lat/0701002].
  - [2] K. Rajagopal and F. Wilczek, arXiv:hep-ph/0011333.
  - [3] D. H. Rischke, Prog. Part. Nucl. Phys. **52**, 197 (2004) [arXiv:nucl-th/0305030].
  - [4] M. Buballa, Phys. Rept. **407**, 205 (2005) [arXiv:hep-ph/0402234].
  - [5] M. G. Alford, A. Schmitt, K. Rajagopal and T. Schafer, arXiv:0709.4635 [hep-ph].
  - [6] M. G. Alford, K. Rajagopal and F. Wilczek, Nucl. Phys. B **537**, 443 (1999) [arXiv:hep-ph/9804403].
  - [7] M. Kitazawa, T. Koide, T. Kunihiro and Y. Nemoto, Prog. Theor. Phys. **108**, 929 (2002) [arXiv:hep-ph/0207255].
  - [8] T. Hatsuda, M. Tachibana, N. Yamamoto and G. Baym, Phys. Rev. Lett. **97**, 122001 (2006) [arXiv:hep-ph/0605018]; Phys. Rev. D **76**, 074001 (2007) [arXiv:0704.2654 [hep-ph]].
  - [9] T. Schafer and F. Wilczek, Phys. Rev. Lett. **82**, 3956 (1999) [arXiv:hep-ph/9811473]; M. G. Alford, J. Berges and K. Rajagopal, Nucl. Phys. B **558**, 219 (1999) [arXiv:hep-ph/9903502].
  - [10] Z. Zhang, K. Fukushima and T. Kunihiro, Phys. Rev. D **79**, 014004 (2009) [arXiv:0808.3371 [hep-ph]].
  - [11] M. Kobayashi and T. Maskawa, Prog. Theor. Phys. **44**, 1422 (1970); M. Kobayashi, H. Kondo and T. Maskawa, Prog. Theor. Phys. **45**, 1955 (1971); G. 't Hooft, Phys. Rev. **D14**, 3432 (1976); Phys. Rep. **142**, 357 (1986).
  - [12] Z. Zhang and T. Kunihiro, Phys. Rev. D **80**, 014015 (2009) [arXiv:0904.1062 [hep-ph]].
  - [13] S. B. Ruester, V. Werth, M. Buballa, I. A. Shovkovy and D. H. Rischke, Phys. Rev. D **72**, 034004 (2005) [arXiv:hep-ph/0503184].
  - [14] H. Abuki and T. Kunihiro, Nucl. Phys. A **768**, 118 (2006) [arXiv:hep-ph/0509172].
  - [15] D. Ebert and H. Reinhardt, Nucl. Phys. B **271**, 188 (1986).
  - [16] V. Bernard, R. L. Jaffe and U. G. Meissner, Phys. Lett. B **198**, 92 (1987).
  - [17] T. Hatsuda and T. Kunihiro, Phys. Lett. B **198**, 126 (1987).
  - [18] T. Kunihiro and T. Hatsuda, Phys. Lett. B **206**, 385 (1988); Erratum-ibid. **210**, 278 (1988); T. Kunihiro, Phys. Lett. B **219**, 363 (1989).



- [19] V. Bernard, R. L. Jaffe and U. G. Meissner, Nucl. Phys. B **308**, 753 (1988).
- [20] P. Rehberg, S. P. Klevansky and J. Hufner, Phys. Rev. C **53**, 410 (1996) [arXiv:hep-ph/9506436].
- [21] M. Huang and I. A. Shovkovy, Phys. Rev. D **70**, 094030 (2004) [arXiv:hep-ph/0408268].